

# CrystEngComm

Accepted Manuscript



This is an *Accepted Manuscript*, which has been through the Royal Society of Chemistry peer review process and has been accepted for publication.

*Accepted Manuscripts* are published online shortly after acceptance, before technical editing, formatting and proof reading. Using this free service, authors can make their results available to the community, in citable form, before we publish the edited article. We will replace this *Accepted Manuscript* with the edited and formatted *Advance Article* as soon as it is available.

You can find more information about *Accepted Manuscripts* in the [Information for Authors](#).

Please note that technical editing may introduce minor changes to the text and/or graphics, which may alter content. The journal's standard [Terms & Conditions](#) and the [Ethical guidelines](#) still apply. In no event shall the Royal Society of Chemistry be held responsible for any errors or omissions in this *Accepted Manuscript* or any consequences arising from the use of any information it contains.

# Graphene oxide as a template for a complex functional oxide

Rebecca Boston<sup>†</sup>, O. Alexander Bell<sup>‡</sup>, Valeska P. Ting, Andrew T. Rhead, Tadachika Nakayama, Charl F. J. Faul and Simon R. Hall\*

*R Boston<sup>†</sup>, Bristol Centre for Functional Nanomaterials, University of Bristol, Bristol, BS8 1FD, UK*

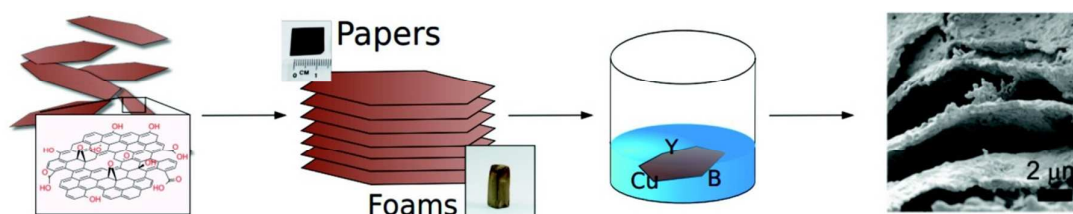
*R. Boston, O. A. Bell, C. F. J. Faul and S. R. Hall, School of Chemistry, University of Bristol, Bristol, BS8 1TS*

*V. P. Ting, Department of Chemical Engineering, University of Bath, Bath, BA2 7AY*

*A. T. Rhead, Department of Mechanical Engineering, University of Bath, Bath, BA2 7AY*

*T. Nakayama, Department of Electrical Engineering, Nagaoka University of Technology, 1603 1 Kamitomioka, Nagaoka, Niigata, 940 2188, Japan*

## Table of contents entry



Graphene oxide monoliths of defined macromorphology are used to direct the structure of complex oxides for improved functionality.



Journal Name

## COMMUNICATION

## Graphene oxide as a template for a complex functional oxide

R. Boston<sup>†a,b</sup>, A. Bell<sup>†b</sup>, V. P. Ting<sup>c</sup>, A. T. Rhead<sup>d</sup>, T. Nakayama<sup>e</sup>, C. F. J. Faul<sup>b</sup> and S. R. Hall<sup>b\*</sup>Received 00th January 20xx,  
Accepted 00th January 20xx

DOI: 10.1039/x0xx00000x

www.rsc.org/

**We report the first use of graphene oxide (GO) as a sacrificial template for the structural direction of complex oxides. The superconductor yttrium barium copper oxide (YBCO) was used as a quaternary oxide test system, with the GO templates being used to create foams and layered paper-like structures which retained the superconducting properties of YBCO.**

The templated synthesis of inorganic materials is an actively researched field,<sup>1,2</sup> with materials for applications such as piezoelectrics,<sup>3</sup> solid oxide fuel cells<sup>4</sup> and photonic crystals<sup>5</sup> all being created using this flexible and wide-ranging technique. The use of biologically-derived templates has yielded a number of hitherto unavailable morphologies in complex oxide materials, such as nanowires,<sup>6,7</sup> microspheres,<sup>8</sup> and more complex structures.<sup>9</sup> Template-based synthesis pathways have also given greater insight into the fundamental mechanisms that govern nanoscale crystal growth.<sup>10</sup> Typically highly carbonaceous and strongly chelating, these templates prevent agglomeration and sintering of stable intermediates during high temperature syntheses. This allows the formation of the desired phase without slow and energy-intensive heating and grinding steps.<sup>11</sup> Thus, templated syntheses are more efficient, whilst still allowing for fine control of phase and morphology.

Whilst nano- and micrometer-scale growth of crystallites using biotemplates is well understood, it is challenging to up-scale this control to create well-ordered macroscopic structures. This is possible by use of a sacrificial template, which directs the morphology at the chosen length scale<sup>12,13</sup> and is destroyed during synthesis, leaving the final inorganic product as a polycrystalline replica.<sup>14,15</sup> This allows, for example, construction of monolithic inverse opaline crystals from simple oxides such as SiO<sub>2</sub> and TiO<sub>2</sub><sup>16</sup> or metals.<sup>17</sup> There are many prior examples of simple oxides

constructed from sacrificial templates, but their use for ternary or quaternary materials, such as complex metal oxides like YBa<sub>2</sub>Cu<sub>3</sub>O<sub>7-δ</sub> (Y123), remains relatively rare.<sup>18–21</sup> Y123 is an excellent model system for testing the efficacy of templating methods in complex oxides due to the strong dependence of the superconducting properties of Y123 upon the templated morphology and phase purity.

Graphene oxide (GO) is a promising material for templating metal oxides, showing effective templating of SiO<sub>2</sub> into a nanoflake morphology.<sup>22</sup> GO consists of single-atom-thick carbon sheets, but differs markedly from graphene. GO contains a random oxygen-rich network of sp<sup>3</sup>-hybridised carbon atoms, interspersed with islands of pristine sp<sup>2</sup>-hybridised graphitic carbon<sup>23,24</sup> (from which GO is initially synthesized). GO is well-known for its flexibility for the creation of different structures such as three-dimensional macroporous solids,<sup>25,26</sup> hydrogels,<sup>27</sup> and papers.<sup>28</sup> As GO starts from an aqueous dispersion, it is able to take on the shape of the vessel in which it is prepared, making it extremely versatile for the creation of bespoke shapes, for example curved structures or porous monoliths. It is also capable of uptake of transition metal ions (for example Cu<sup>2+</sup>) from solution.<sup>29</sup> The wide variety of available final morphologies from a single material,<sup>30</sup> combined with an abundance of chelating hydroxyl and ketone functionalities,<sup>24,31</sup> makes GO attractive for use as a template for oxide materials.

Here we present the first instance of GO-templating of a quaternary metal oxide and demonstrate the use of monolithic GO templates to produce, in this case, the complex oxide Y123. Two morphologies of GO (foam and paper) were chosen; both were synthesized from GO aqueous solutions by previously reported methods<sup>25,28</sup> and were successfully used to control and direct the growth of highly crystalline superconducting Y123 structures with highly porous, or oriented structures, respectively. The resulting Y123 materials demonstrate an improvement in critical current density of the superconducting phase when compared with solid-state synthesis,<sup>32,33</sup> and act as proof of concept that GO can be used as a template for complex oxides.

Full details of the experimental methods can be found in the supporting information, but briefly, monolithic GO structures with foam and layered paper-like microstructure were immersed in aqueous solutions of Y, Ba, and Cu nitrate salts. Soaked templates were then dried and calcined to obtain templated YBCO. Initially the structure of the template and inorganic replicas were investigated

<sup>a</sup> Bristol Centre for Functional Nanomaterials, Centre for Nanoscience and Quantum Information, University of Bristol, Tyndall Avenue, Bristol BS8 1FD, UK

<sup>b</sup> School of Chemistry, University of Bristol, Cantock's Close, Bristol, BS8 1TS, UK

<sup>c</sup> Department of Chemical Engineering, University of Bath, Bath, BA2 7AY, UK

<sup>d</sup> Department of Mechanical Engineering, University of Bath, Bath, BA2 7AY, UK

<sup>e</sup> Department of Electrical Engineering Nagaoka University of Technology, 1603 1 Kamitomioka, Nagaoka, Niigata, 940 2188, Japan

Electronic Supplementary Information (ESI) available: Full experimental details, TEM, electron diffraction, powder XRD, and critical current density plots.

See DOI: 10.1039/x0xx00000x

†These authors contributed equally.

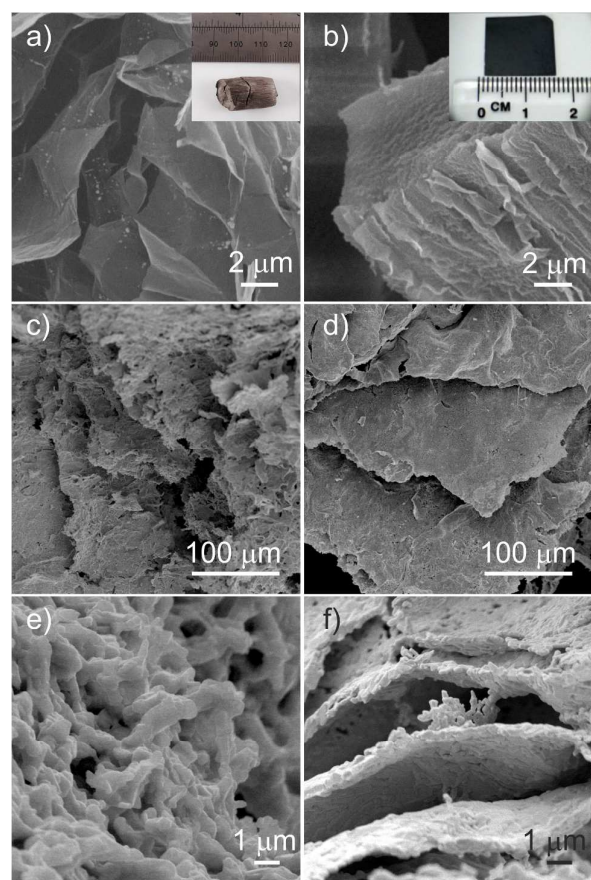


Figure 1. SEM micrographs of a) foam and b) paper templates prior to combination with the precursor solution, with inset photographs of each. c) and d) show micrographs of the calcined Y123 foam and layered structure respectively, with the microstructures shown in e) and f). The macroscopic structure of the GO is retained between the uncalcined (a and b) and calcined samples (c-f), in particular the layers in the GO paper which can be clearly seen in d and f.

using SEM, as shown in Figure 1. Figure 1a and Figure 1b show SEM micrographs of the GO foam and paper respectively, prior to soaking in the precursor, with inset photographs showing the macroscopic monoliths. SEM micrographs of the two templated solid structures (Figure 1c-f) show excellent retention of the templates' porous (foam) and highly layered (paper) structures, respectively. The templated products show a polycrystalline structure, arranged in the same morphology and microstructure as the GO templates.

Non-destructive imaging by X-ray micro-computed tomography (X-ray  $\mu$ -CT) revealed an interconnected macroporous internal structure (Figure 2). Figure 2a shows a model of the macropores present within a small section of the Y123 foam, with Figure 2b showing a cut-away of the sample illustrating the micron-scale porous internal structure. This structure is a good replica of the GO template, and indicates that the porous structure is retained throughout the sample during calcination. The pore mapping was used to obtain an average porosity of 42%. The structure of the paper-like Y123 is displayed in Figure 2c, with Figure 2d showing the layered structure is present throughout the sample, imparted by the GO template.

The composition of both the foam- and paper-templated Y123 was determined using TEM/EDX (Figure S1) and powder X-ray diffraction (Figure S2). The majority phase in both the foam and paper-templated Y123 is

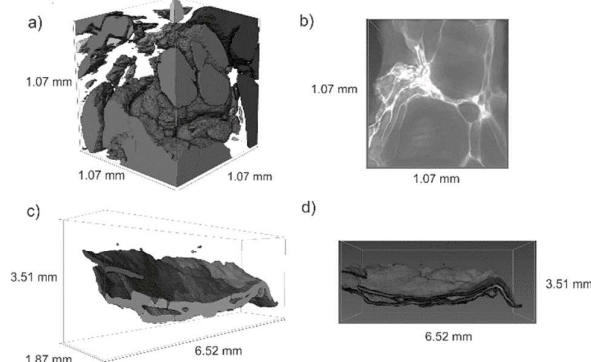


Figure 2. X-ray  $\mu$ -CT images of a) and b) the Y123 foam showing, respectively, internal macro-pore structure and solid pore walls, and c) and d) the Y123 paper showing, respectively, internal layered structure and detailed morphology.

$\text{YBa}_2\text{Cu}_3\text{O}_{6.9}$  (JCPDS card 79-0653), which is consistent with optimal oxygenation. A small number of impurity phases were also observed, including  $\text{CuO}$ ,  $\text{BaCuO}_2$  and  $\text{Y}_2\text{BaCuO}_5$ .

Central to the success of any templated system is the mechanism by which the template acts to produce the final product (in this case Y123). This can be considered in two ways- the chemical pathway and the physical direction of crystallites imparted by the template. The chemical pathway for the formation of Y123 was investigated with a series of increasing calcination temperatures. Figure 3 shows the indexed PXRD patterns of samples heated to temperatures between 200 °C and 900 °C (at 100 °C intervals) and suggests that this synthesis proceeds *via* a different low-temperature pathway to that which has been observed previously with some polysaccharide biotemplates.<sup>10–12</sup> The synthesis does, however, show some similarities to the high carbon-content dextran-based syntheses,<sup>8</sup> as might be expected given the high carbon content of GO.

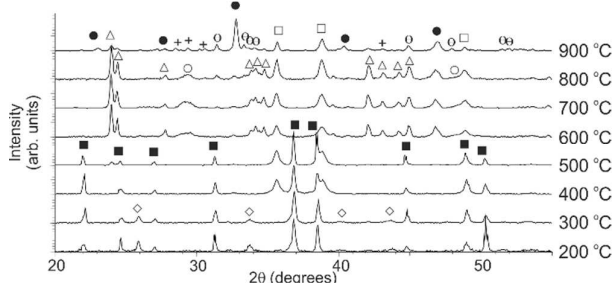


Figure 3. Temperature study of the formation of the Y123 phase. Phases present are  $\text{Ba}(\text{NO}_3)_2$  (■),  $\text{Cu}(\text{NO}_3)_2(\text{H}_2\text{O})_3$  (◊),  $\text{YBa}_2\text{Cu}_3\text{O}_{6.9}$  (●),  $\text{CuO}$  (□),  $\text{BaCO}_3$  (Δ),  $\text{Y}_2\text{O}_3$  (○),  $\text{BaCuO}_2$  (+) and  $\text{Y}_2\text{Cu}_2\text{O}_5$  (◊).

At 200 °C, the major crystalline phases present are the precursor materials barium and copper nitrates (JCPDS cards 76-1376 and 45-0594 respectively). As fully chelated ions are non-crystalline and therefore do not appear in the XRD pattern, the presence of these crystalline phases at these low temperatures is due to recrystallization of excess precursor solution present on the surface of the template upon drying. Barium nitrate is observed in greater quantities than the other two ions due to the fact that yttrium nitrate thermally decomposes below 200 °C, and copper



nitrate between 200 °C and 300 °C (accounting for the small quantities observed at these temperatures).

Between 300 °C and 400 °C the copper ions chelated in the monolith react with the template to form copper (II) oxide (JCPDS card 74-1021) which, crucially, allows for the retention of the

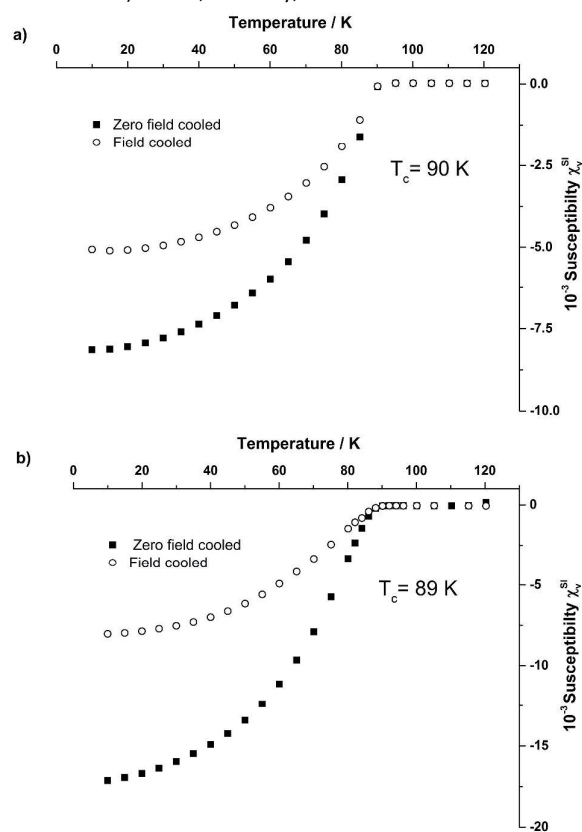


Figure 4. SQUID magnetometry showing superconducting transition temperature,  $T_c$ , of a) Y123 foam and b) paper Y123.

template structure while the desired inorganic phase forms. Between 400 °C and 600 °C, as the template fully decomposes, the  $\text{Ba}^{2+}$  and  $\text{Y}^{3+}$  ions react to form yttrium oxide and barium carbonate (JCPDS cards 74-1828 and 41-0373 respectively), which are homogeneously spread throughout the material.

The next significant change in the sample occurs in the 800 °C and 900 °C interval, where a solid-solid reaction between  $\text{Y}^{3+}$ ,  $\text{Ba}^{2+}$  and  $\text{Cu}^{2+}$  ions occurs due to the decomposition of  $\text{BaCO}_3$  above 811 °C. Here again, the fact that the template is perfectly replicated indicates that the reaction to form the final product is occurring in the solid state, and as is observed in templates such as dextran,<sup>21</sup> the final Y123 product only forms where the template has been. In this templated approach, however, the time over which this reaction occurs is reduced to two hours due to the higher degree of mixing between the three precursor ions provided by the chelating template. The synthesis then proceeds as observed previously in typical biotemplated systems,<sup>8,34</sup> with Y123 emerging as the major phase between 800 °C and the final calcination temperature, 920 °C. Small quantities of  $\text{Y}_2\text{Cu}_2\text{O}_5$  (JCPDS card 33-0511) and  $\text{BaCuO}_2$  (JCPDS card 70-0441) are also observed at 900 °C, indicating that the final formation of the Y123 phase is dependent on both the higher final temperature (920 °C) and a longer hold time than was used in the temperature study. By holding the samples at 920 °C for

two hours, the quantity of these small impurity phases were reduced (Figure S2).

SQUID magnetometry of the templated Y123 was performed to determine the transition temperature,  $T_c$  (Figure 4) and critical current density,  $J_c$  (Figure S3) of the templated Y123. Transition temperatures of  $90 \pm 1$  K and  $89 \pm 1$  K were measured for the foam and paper morphologies, respectively, close to the optimum value for  $T_c$  in Y123. The critical current densities were determined at 1 T applied field and 10 K. Values were measured to be  $0.10 \text{ MA cm}^{-2}$  (foam) and  $0.05 \text{ MA cm}^{-2}$  (layered). The difference between values the foam and paper-like samples can be attributed to the greater continuity of the crystallites in the foam sample- the greater number of interconnects between crystallites results in there being more pathways in which the supercurrent can flow, resulting in a larger critical current density being measured. Conversely the paper-like structure, being composed of layers, has these same crystallite connections in only two dimensions, resulting in a lower value measure for  $J_c$ .

These values are greater than previously reported values of  $J_c$  for commercially available polycrystalline Y123, which are of the order  $0.02 \text{ MA cm}^{-2}$ .<sup>21</sup> Whilst the values obtained are lower than those known for industrial Y123<sup>35</sup> we believe the templated synthesis technique presented here has the advantage of allowing customization of the morphology of quaternary metal oxides such as YBCO to suit specific applications, while maintaining a good material quality.

In conclusion, we have successfully exploited a novel and highly modifiable template for the construction of oxide materials with pre-determined micro-scale structure, illustrated by the creation of superconducting oxide monoliths. We have shown that, due to low temperature stable intermediate phase formation, the final product faithfully retains the structure of the uncalcined GO template, allowing porous foams and highly layered oxide structures to be created. With many further GO morphologies available, this template has potential for great utility in obtaining application-specific morphologies, e.g. foams for rapid access of cryogenics to improve cool-down times in superconductors, which retain the desired properties. We have also elucidated the crystallochemical mechanism by which template allows formation of the Y123 phase. This work demonstrates that GO deserves a place alongside biotemplates in the arsenal of options available for creating highly ordered functional inorganic materials.

## Acknowledgements

AB, RB and SRH acknowledge the Engineering and Physical Sciences Research Council (EPSRC), UK (grant EP/G036780/1), and, RB and SRH the Bristol Centre for Functional Nanomaterials for project funding. All authors would like to acknowledge the Electron and Scanning Probe Microscopy Facility at the School of Chemistry, University of Bristol for the use of electron microscopes. VPT thanks the University of Bath for funding via a Prize Fellowship. CFJF thanks the University of Bristol for support.

## Notes and references

- 1 Z. Schnepf, *Angew. Chem. Int. Ed.*, 2013, **52**, 1096.
- 2 H. Zhou, T. Fan and D. Zhang, *ChemSusChem*, 2011, **4**, 1344.
- 3 Z. Schnepf, J. Mitchells, S. Mann and S. R. Hall, *Chem. Commun.*, 2010, **46**, 4887.

- 4 D. Dong, Y. Wu, X. Zhang, J. Yao, Y. Huang, D. Li, C.-Z Li and H. Wang, *J. Mater. Chem.*, 2011, **21**, 1028.
- 5 M. J. Jorgensen and M. H. Bartl, *J. Mater. Chem.*, 2011, **21**, 10583.
- 6 K. Cung, B. J. Han, T. D. Nguyen, S. Mao, Y.-W. Yeh, S. Xu, R. R. Naik, G. Poirier, N. Yao, P. K. Purohit and M. C. McAlpine, *Nano Lett.*, 2013, **13**, 6197.
- 7 M.-Y. Chang, W.-H. Wang and Y.-C. Chung, *J. Mater. Chem.*, 2011, **21**, 4966.
- 8 R. Boston, A. Carrington, D. Walsh, and S. R. Hall, *CrystEngComm*, 2013, **15**, 3763.
- 9 J. M. Galloway, J. P. Bramble, A. E. Rawlings, G. Burnell, S. D. Evans and S. Staniland, *Small*, 2012, **8**, 204.
- 10 R. Boston, Z. Schnepf, Y. Nemoto, Y. Sakka, and S.R. Hall, *Science*, 2014, **344**, 623.
- 11 A. Dermont, M. S. Dyer, R. Sayers, M. F. Thomas, M. Tsiamtsouri, H. N. Niu, G. R. Darling, A. Daoud-Aladine, J. B. Claridge and M. J. Rosseinsky, *Chem. Mater.*, 2010, **22**, 6598.
- 12 T. T. Vu and G. Marb  n, *App. Cat. B*, 2014, **152-3**, 51.
- 13 M. K. Mayeda, J. Hayat, T. H. Epps and J. Lauterbach, *J. Mater. Chem. A*, 2015, **3**, 7822.
- 14 R. Banerjee, H. Furukawa, D. Britt, C. Knobler, M. O'Keeffe and O. M. Yaghi, *J. Am. Chem. Soc.*, 2009, **131**, 3875.
- 15 A. A. Voskanyan, C.-Y. V. Li, K.-Y. Chan and I. Gao, *CrystEngComm*, 2015, **17**, 2620.
- 16 G. I. N. Waterhouse and M. R. Waterland, *Polyhedron*, 2007, **26**, 356.
- 17 K. M. Kulinowski, P. Jiang, H. Vaswani and V. L. Colvin, *Adv. Mater.*, 2000, **12**, 833.
- 18 E. Culverwell, S. C. Wimbush and S. R. Hall, *Chem. Commun.*, 2008, **9**, 1055.
- 19 D. C. Green, M. R. Lees and S. R. Hall, *Chem. Commun.*, 2013, **49**, 2974.
- 20 E. S. Reddy, J. G. Noudem and C. Goupil, *Energy Convers. Manag.*, 2007, **48**, 1251.
- 21 D. Walsh, S. C. Wimbush and S. R. Hall, *Chem. Mater.*, 2007, **19**, 647.
- 22 Z. Lu, J. Zhu, D. Sim, W. Zhou, W. Shi, H. H. Hng and Q. Yan, *Chem. Mater.*, 2011, **23**, 5293.
- 23 A. Lerf, H. He, M. Forster and J. Klinowski, *J. Phys. Chem. B*, 1998, **102**, 4477.
- 24 K. Erickson, R. Erni, Z. Lee, N. Alem, W. Gannett and A. Zettl, *Adv. Mater.*, 2010, **22**, 4467.
- 25 L. Qiu, J. Z. Liu, S. L. Y. Chang, Y. Wu and D. Li, *Nat. Commun.*, 2012, **3**, 1241.
- 26 J. L. Vickery, A. J. Patil and S. Mann, *Adv. Mater.*, 2009, **21**, 2180.
- 27 H. Bai, C. Li, X. Wang and G. Shi, *Chem. Commun.*, 2010, **46**, 2376.
- 28 D. A. Dikin, S. Stankovich, E. J. Zimney, R. D. Piner, G. H. B. Dommett, G. Evmenenko, S. T. Nguyen and R. S. Ruoff, *Nature*, 2007, **448**, 457.
- 29 X. Mi, G. Huang, W. Xie, W. Wang, Y. Liu and J. Gao, *Carbon*, 2012, **50**, 4856.
- 30 H.-P. Cong, J.-F. Chen and S.-H Yu, *Chem. Soc. Rev.*, 2014, **43**, 7295.
- 31 A. M. Dimiev, L. B. Alemany and J. M. Tour, *ACS Nano*, 2013, **7**, 576.
- 32 H. S  zeri, H.   zkan, and N. Ghazanfari, *J. Alloys Compd.*, 2007, **428**, 1.
- 33 A. Usoskin, J. Dzick, A. Issaev, J. Knoke, F. Garc  , F. Garc  a-Moreno, K. Sturm and H. C. Freyhardt, *Supercond. Sci. Technol.*, 2001, **14**, 676.
- 34 D. Larbalestier, A. Gurevich, D. M. Feldmann, and A. Polyanskii, *Nature*, 2001, **414**, 368.
- 35 Z. A. C. Schnepf, S. C. Wimbush, S. Mann and S. R. Hall, *Adv. Mater.*, 2008, **20**, 1782.